Supplementary information

Supplementary figures

Table S1-8

Figure S1

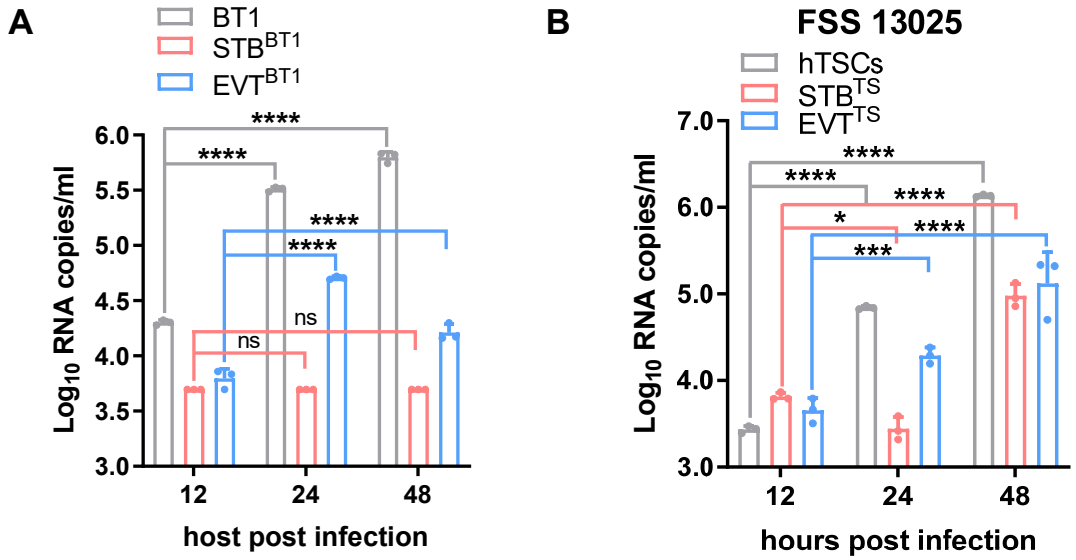

Figure S1. Detection of ZIKV RNA in the supernatants of ZIKV-infected hTSC-derived trophoblast cells.

(A) Quantification of ZIKV RNA in the supernatants of BT1, STB^{BT1} and EVT^{BT1} at 12, 24 and 48 hours post infection. The BT1, STB^{BT1} and EVT^{BT1} were infected with ZIKV at an MOI of 0.1. Two-way ANOVA analysis was used for statistical analysis of significance. n=3 independent experiments. ****, $p<0.0001$. ns, no significance.

(B) Quantification of ZIKV RNA in the supernatants of hTSCs, STB^{TS} and EVT^{TS} at 12, 24 and 48 hours post infection. The hTSCs, STB^{TS} and EVT^{TS} were infected with ZIKV strain FSS 13025 at an MOI of 0.1. Two-way ANOVA analysis was used for statistical analysis of significance. n=3 independent experiments. STB^{TS}, 12 hpi vs 24 hpi, *, $p=0.18$. EVT^{TS}, 12 hpi vs 24 hpi, ***, $p=0.0002$. ****, $p<0.0001$.

Data in this figure are shown as the mean ± s.d.

Figure S2

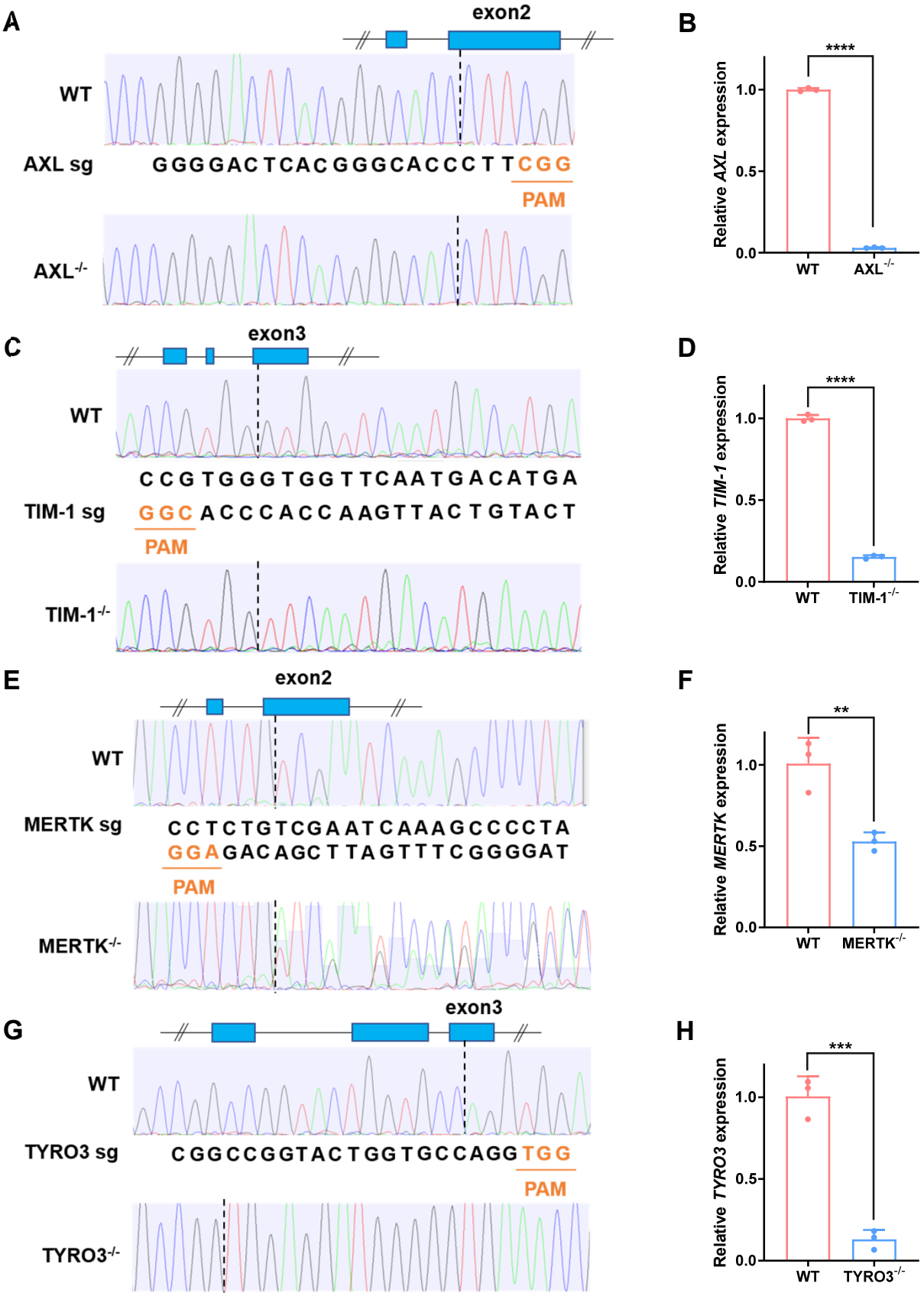

Figure S2. Knockout of AXL, TIM-1, MERTK and TYRO3 in hTSCs using CRISPR/Cas9 system.

(A, C, E, and G) Sanger sequencing results of sgRNA target sites in wildtype (WT), AXL$^{-/-}$ (panel A), TIM-1$^{-/-}$ (panel C), MERTK$^{-/-}$ (panel E) and TYRO3$^{-/-}$ (panel G) hTSCs. (B, D, F, and H) Quantification of AXL, TIM-1, TYRO3, and MERTK mRNA expression in WT, AXL$^{-/-}$ (panel B), TIM-1$^{-/-}$ (panel D), MERTK$^{-/-}$ (panel F) and TYRO3$^{-/-}$ (panel H) hTSCs. Two-tailed unpaired t test was used for statistical analysis of significance. n=3 independent experiments. Panel F, **, p=0.0079. Panel H, ***, p=0.0004. ****, p<0.0001. Data in this figure are shown as the mean ± s.d.

Figure S3

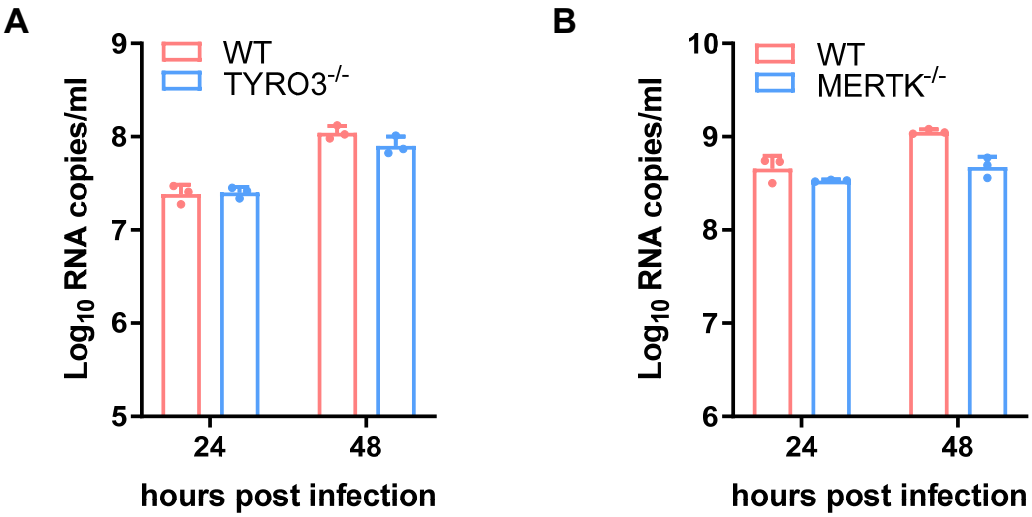

Figure S3. Growth of ZIKV RNA in the supernatants of ZIKV-infected WT, TYRO3$^{-/-}$ and MERTK$^{-/-}$ hTSCs.

(A and B) Quantification of ZIKV RNA in the supernatants of ZIKV-infected WT, TYRO3$^{-/-}$ (panel A) and MERTK$^{-/-}$ (panel B) hTSCs. The cells were exposed to ZIKV infection at an MOI of 0.1, and analyzed at 24 and 48 hours post infection. n=3 independent experiments. Data in this figure are shown as the mean ± s.d.

Figure S4

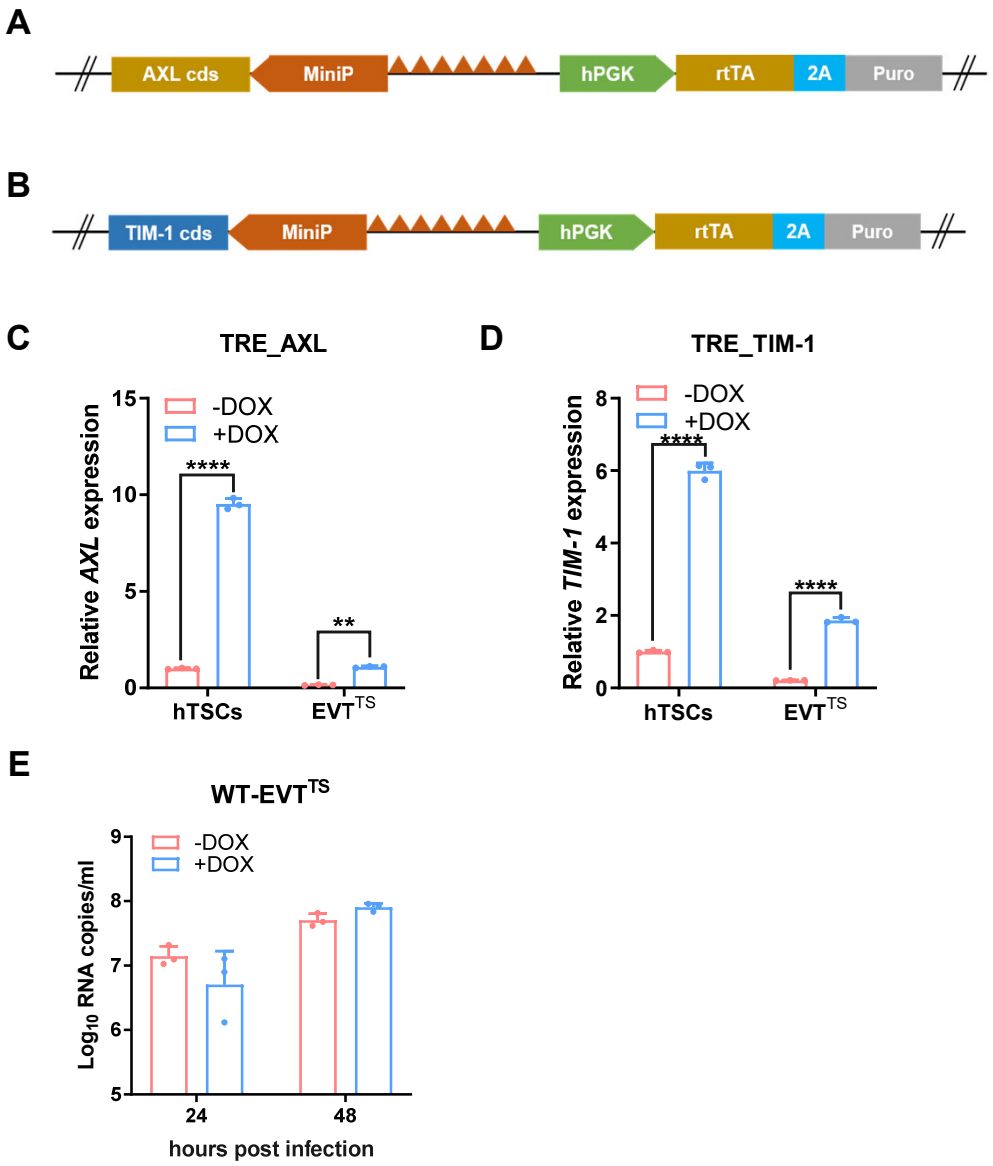

Figure S4. Overexpression of AXL and TIM-1 in EVT^{TS}.

(A and B) The lentiviral vectors used for DOX-induced overexpression of AXL (A) or TIM-1 (B) in EVT^{TS}. MiniP, mini promoter. ▲, tet operator. rtTA, a reverse transcriptional activator. 2A, P2A self-cleaving peptide. Puro, puromycin selection marker.

(C) Quantification of AXL expression in TRE_AXL-hTSCs and TRE_AXL-EVT^{TS} under DOX induction. Two-way ANOVA analysis was used for statistical analysis of significance. n=3 independent experiments. **, p=0.0037. ****, p<0.0001.

(D) Quantification of TIM-1 expression in TRE_TIM-1-hTSCs and TRE_TIM-1-EVT^{TS} under DOX induction. Two-way ANOVA analysis was used for statistical analysis of significance. n=3 independent experiments. ****, p<0.0001.

(E) Quantification of viral RNA in the supernatants of ZIKV-infected WT-EVT^{TS} at 24 and 48 hours post infection. The WT-EVT^{TS} was exposed to ZIKV at MOI 0.1. n=3 independent experiments.

Date in this figure are shown as the mean ± s.d.

Figure S5

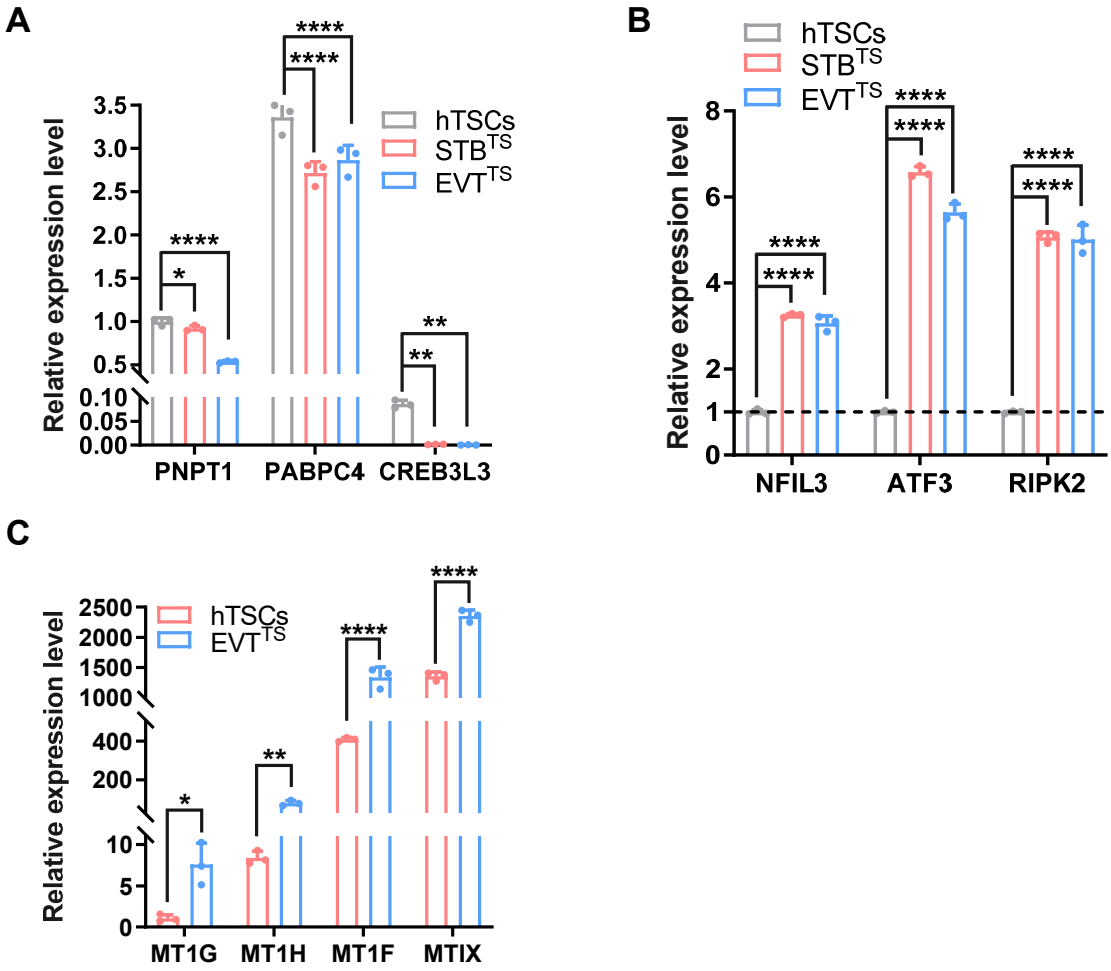

Figure S5. qRT-PCR analysis of the ISG expression in hTSCs, STB^{TS} and EVT^{TS}.

(A) Quantification of PNPT1, PABPC4 and CREB3L3 mRNA expression in hTSCs, STB^{TS} and EVT^{TS}. n=3 independent experiments. Two-way ANOVA analysis was used for statistical analysis of significance. PNPT1, hTSCs vs STB^{TS}, *, p=0.0114. CREB3L3, hTSCs vs STB^{TS}, **, p=0.0079. hTSCs vs EVT^{TS}, **, p=0.0072. ****, p<0.0001.

(B) Quantification of NFIL3, ATF3 and RIPK2 mRNA expression in hTSCs, STB^{TS} and EVT^{TS}. n=3 independent experiments. The dashed line indicates the expression of the genes in hTSCs for normalization. Two-way ANOVA analysis was used for statistical analysis of significance. ****, p<0.0001.

(C) Quantification of MT1G, MT1H, MTIF and MT1X mRNA expression in hTSCs and EVT^{TS}. n=3 independent experiments. Two-way ANOVA analysis was used for statistical analysis of significance. *, p=0.0374. **, p=0.0066. ****, p<0.0001.

Data in this figure are shown as the mean ± s.d.

Figure S6

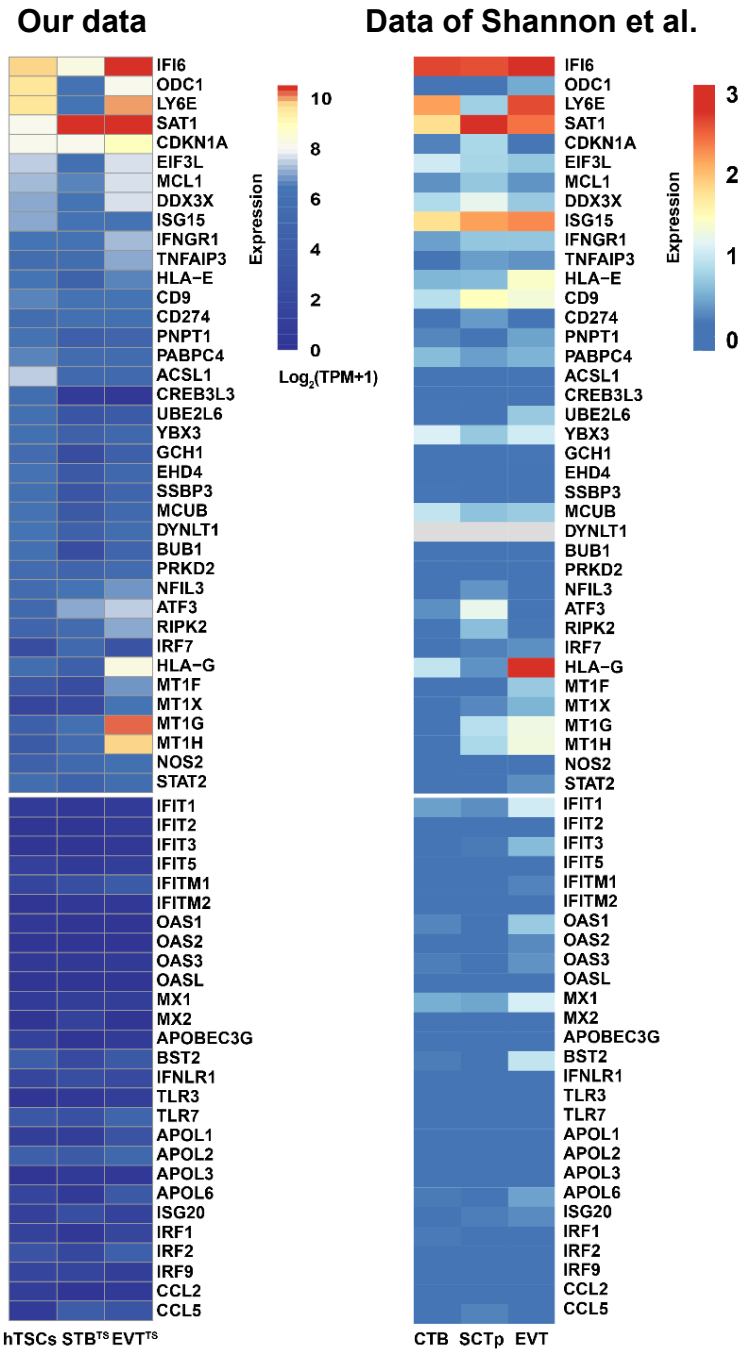

Figure S6. The relative expression of ISGs in hTSCs/CTB, STB^{TS}/SCTp and EVT^{TS}/EVT of our and competing models.

Heatmap showing the relative expression of ISGs with high (up) and low (bottom) expression in our hTSCs, STB^{TS} and EVT^{TS} (left panel), and in CTB, SCTp and EVT of competing models (right panel).

Figure S7

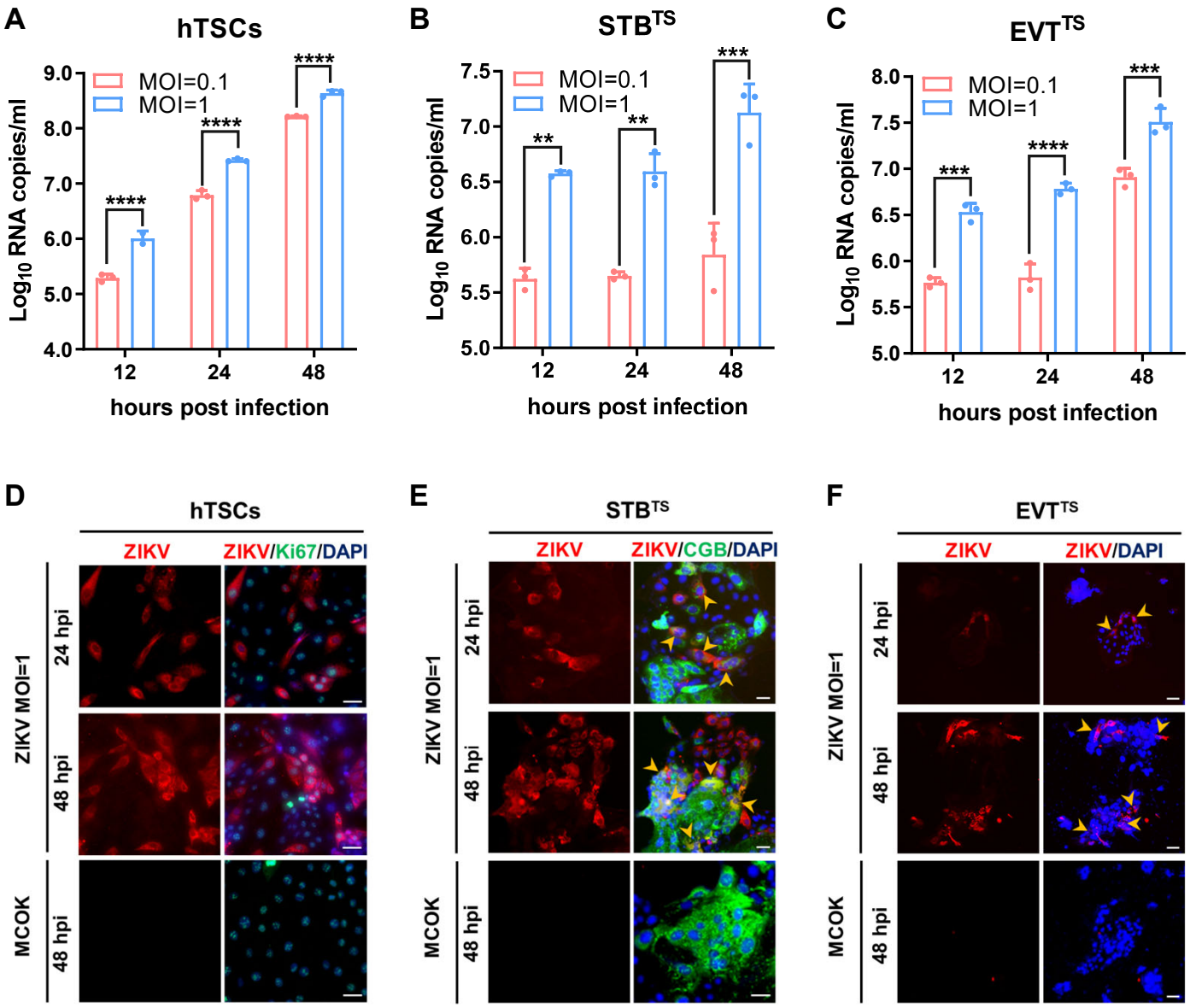

Figure S7. Comparison of the ZIKV infection features of the hTSCs, STB^{TS} and EVT^{TS} infected with ZIKV at MOI 0.1 and 1.

(A, B and C) Quantification of ZIKV RNA in the supernatants of hTSCs (panel A), STB^{TS} (panel B) and EVT^{TS} (panel C) at 12, 24 and 48 hours post infection. The hTSCs, STB^{TS} and EVT^{TS} were infected with at MOIs of 0.1 and 1. Two-way ANOVA analysis was used for statistical analysis of significance. n=3 independent experiments. Panel B, 12 hpi, MOI=0.1 vs MOI=1, **, p=0.0032. 24 hpi, MOI=0.1 vs MOI=1, **, p=0.0034. 48 hpi, MOI=0.1 vs MOI=1, ***, p=0.0006. Panel C, 12 hpi, MOI=0.1 vs MOI=1, ***, p=0.0001. 48 hpi. MOI=0.1 vs MOI=1, ***, p=0.0005. ****, p<0.0001.

(D, E and F) Immunofluorescence staining for Ki67 (a marker of proliferative CTB), CGB (a marker of STB) and ZIKV E protein in hTSCs (panel D), STB^{TS} (panel E) and EVT^{TS} (panel F). Nuclei were stained with DAPI. The hTSCs, STB^{TS} and EVT^{TS} were infected with ZIKV at an MOI of 1 and analyzed at 24 and 48 hours post infection. The yellow arrow heads indicated the positive intracellular ZIKV E signals in STB^{TS} and EVT^{TS}. Scale bars: 50 μm.

Data in this figure are shown as the mean ± s.d.

Figure S8

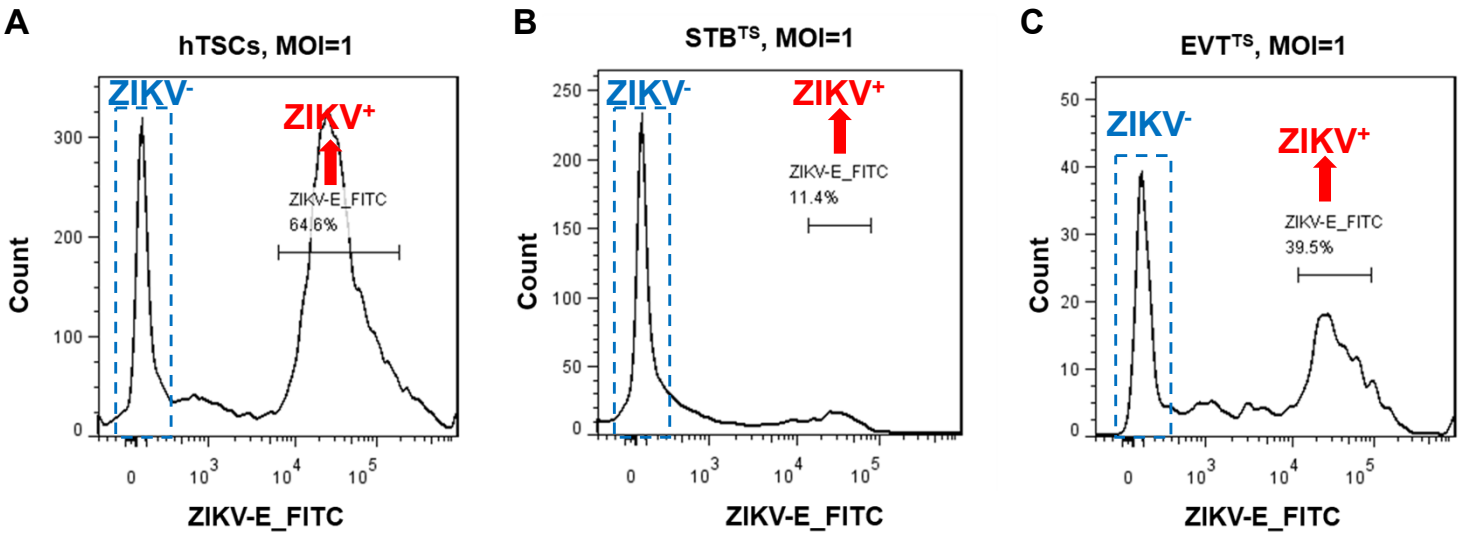

Figure S8. FACS analysis of ZIKV-infected hTSCs, STB^{TS} and EVT^{TS}.
(A, B and C) FACS analysis of ZIKV-infected hTSCs (panel A), STB^{TS} (panel B) and EVT^{TS} (panel C) using ZIKV E protein antibody. The hTSCs, STB^{TS} and EVT^{TS} were infected with ZIKV at MOI 1 and analyzed at 48 hours post infection. Cells were stained for viral E protein and sorted into ZIKV-infected (ZIKV$^{+)}$ and uninfected (ZIKV^{-}) cells. Total RNA of ZIKV^{+} and ZIKV^{-} cells was extracted for qRT-PCR analysis.

Figure S9

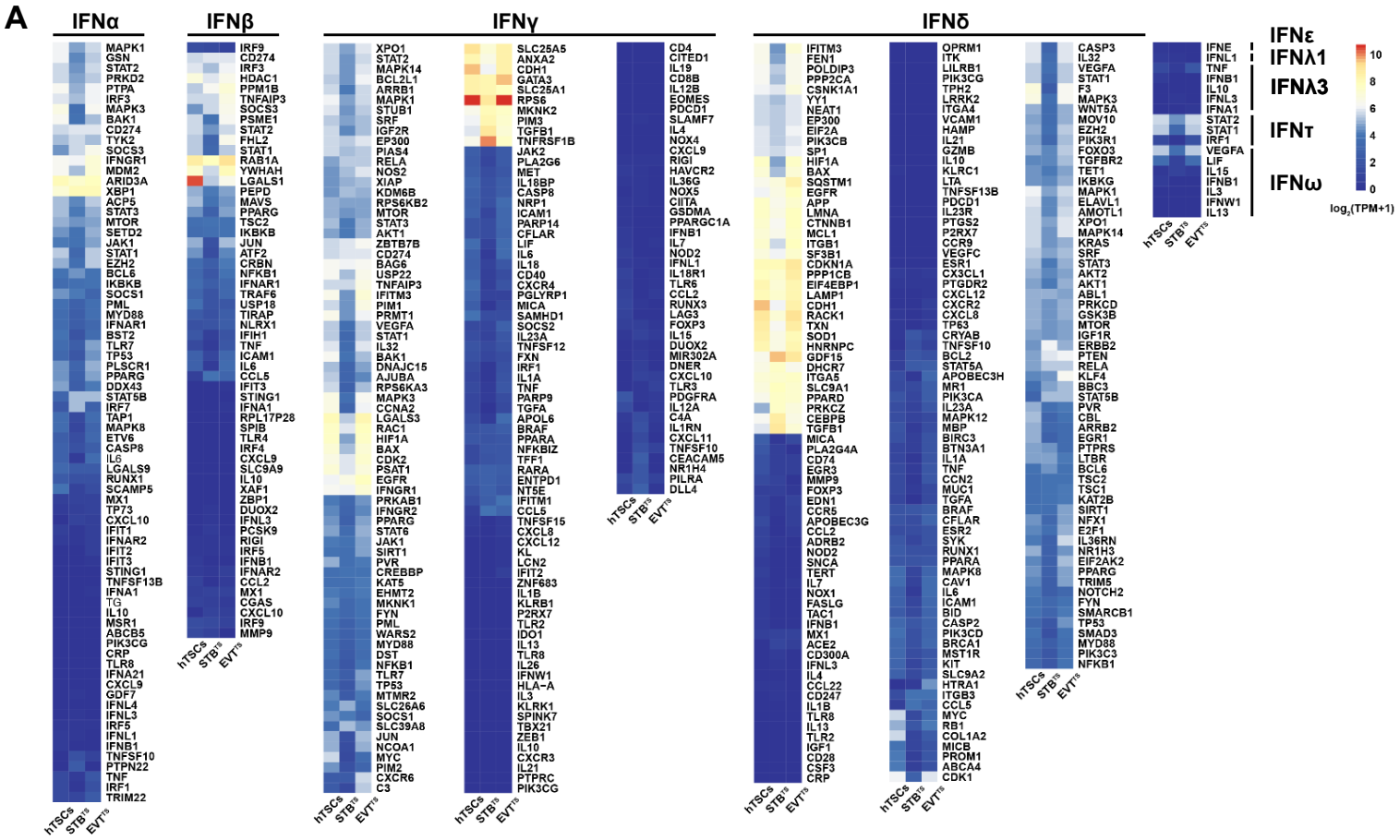

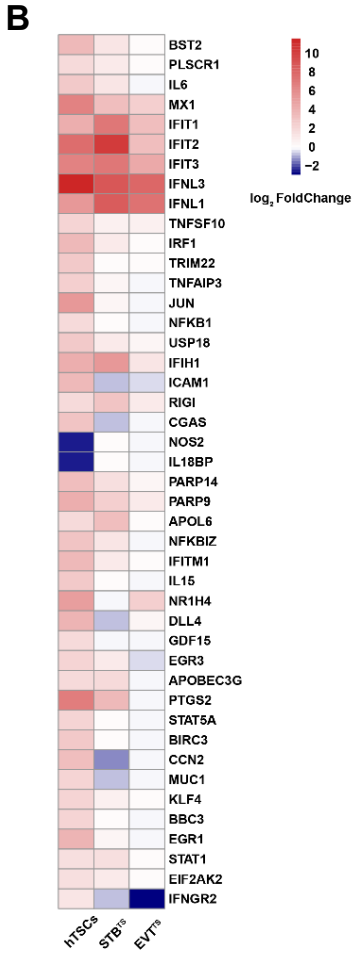

Figure S9. The relative expression of IFNs in mock- and ZIKV-infected hTSCs, STB^{TS} and EVT^{TS}.

(A) Heatmap showing the z-acore TPM of IFNs in hTSCs, STB^{TS} and EVT^{TS}.

(B) Heatmap showing changed IFNs in ZIKV-infected hTSCs, STB^{TS} and EVT^{TS}.

Figure S10

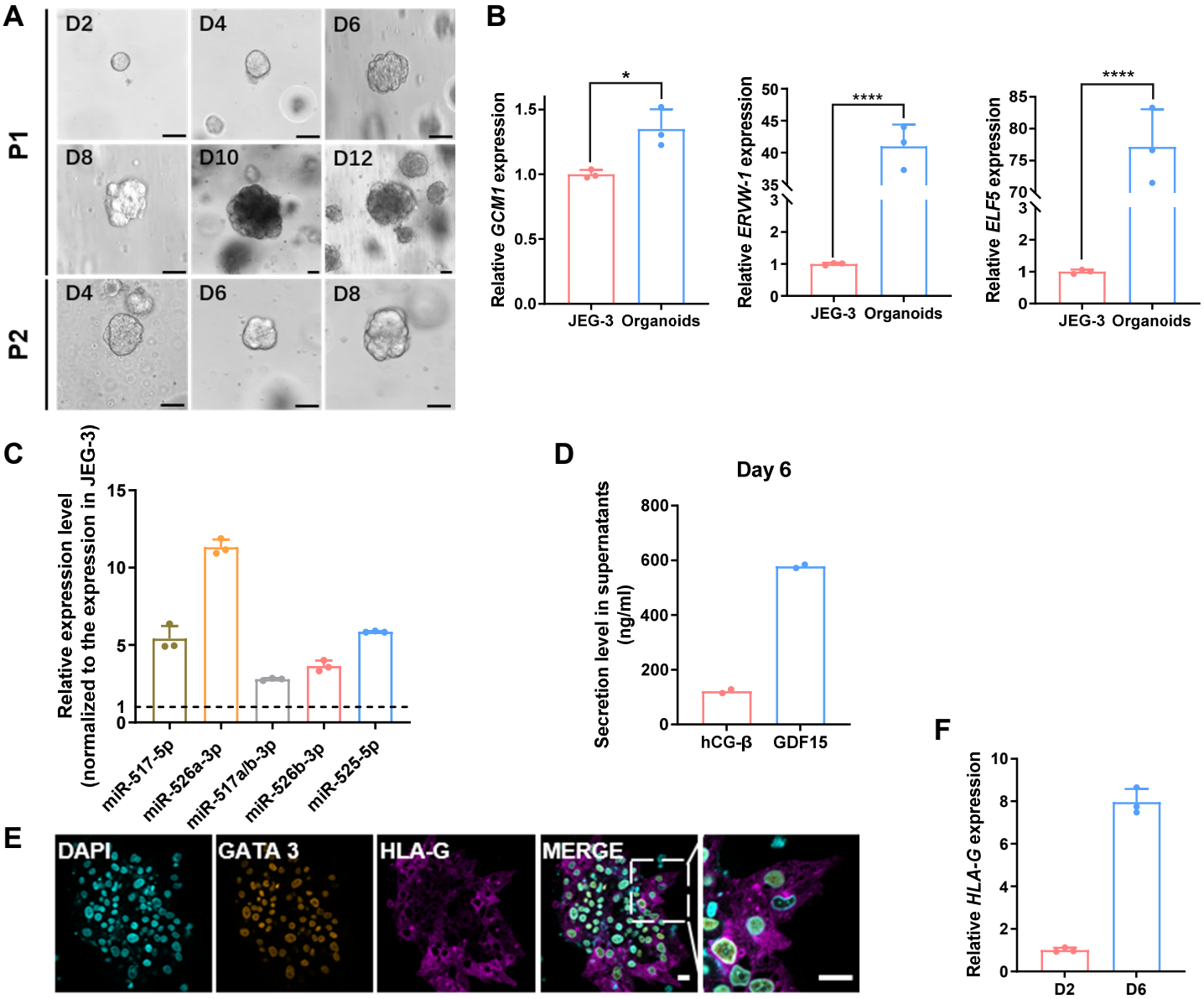

Figure S10. Molecular characterizations of hTSC-organoids.

(A) Brightfield images of passage 1 (P1) and passage 2 (P2) hTSC-organoids. D, Day. Scale bars: 50 μm.

(B) Quantification of GCM1, ERVW-1, and ELF5 mRNA expression in the choriocarcinoma line JEG-3 (positive controls) and hTSC-organoids. Two-tailed unpaired t test was used for statistical analysis of significance. n=3 independent experiments. Left panel, *, p=0.0177. ****, p<0.0001.

(C) Quantification of miRNAs miR-517-5p, miR-526a-3p, miR-517a/b-3p, miR-526b-3p, and miR-525-5p expression in the choriocarcinoma line JEG-3 (positive controls) and hTSC-derived organoids. Graph showing the relative expression levels of the miRNAs from in organoids to those of JEG-3. The dashed line indicates the expression of the genes in JEG-3 for normalization. n=3 independent experiments.

(D) Quantification of the hCG-β and GDF15 secreted by hTSC-organoids by ELISA. The amount of hCG-β and GDF15 secreted by organoids at day 6 was shown. n=2 independent experiments.

(E) Immunofluorescence staining for GATA 3 and HLA-G in the EVT cells derived from hTSC-organoids. Nuclei were stained with DAPI. Scale bars: 20 μm.

(F) Quantification of HLA-G mRNA expression in the hTSC-organoid-derived EVT at day 2 and day 6 after induction. n=3 independent experiments.

Data in panel B, C and F are shown as the mean ± s.d. Data in panel D are shown as mean.

Figure S11

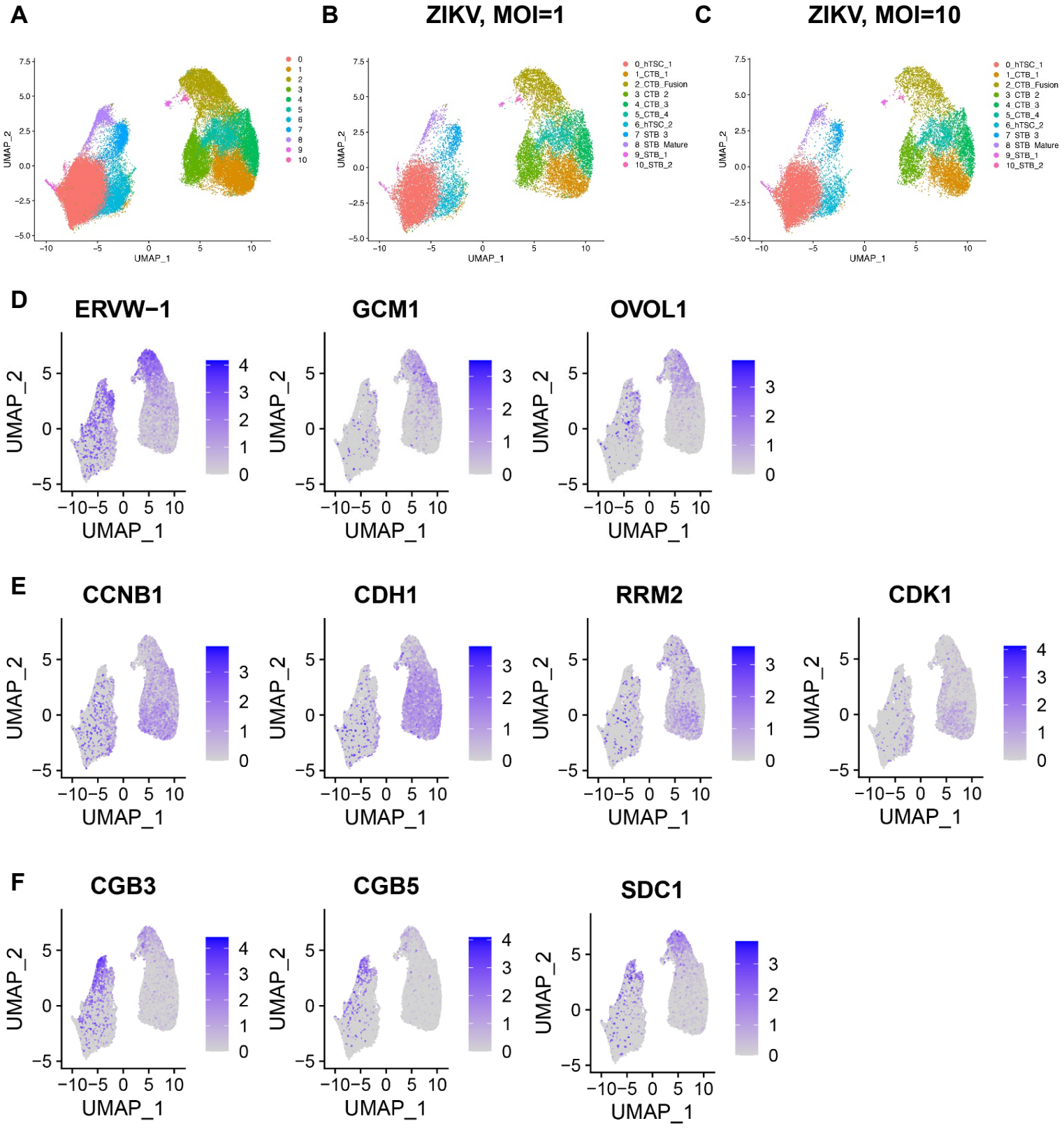

Figure S11. The transcriptome profile of ZIKV-infected hTSC-organoids at single-cell resolution.

(A) UMAP showing the integrated datasets of MOCK- and ZIKV-infected hTSC-organoids.

(B) UMAP showing the cell composition of ZIKV-infected hTSC-organoids. The hTSC-organoids were infected with ZIKV at MOIs of 1 (left panel) and 10 (right panel).

(D, E and F) UMAP showing the cells expressing CTB_Fusion (panel D), CTB (panel E) and STB (panel F) marker genes in hTSC-organoids.

Figure S12

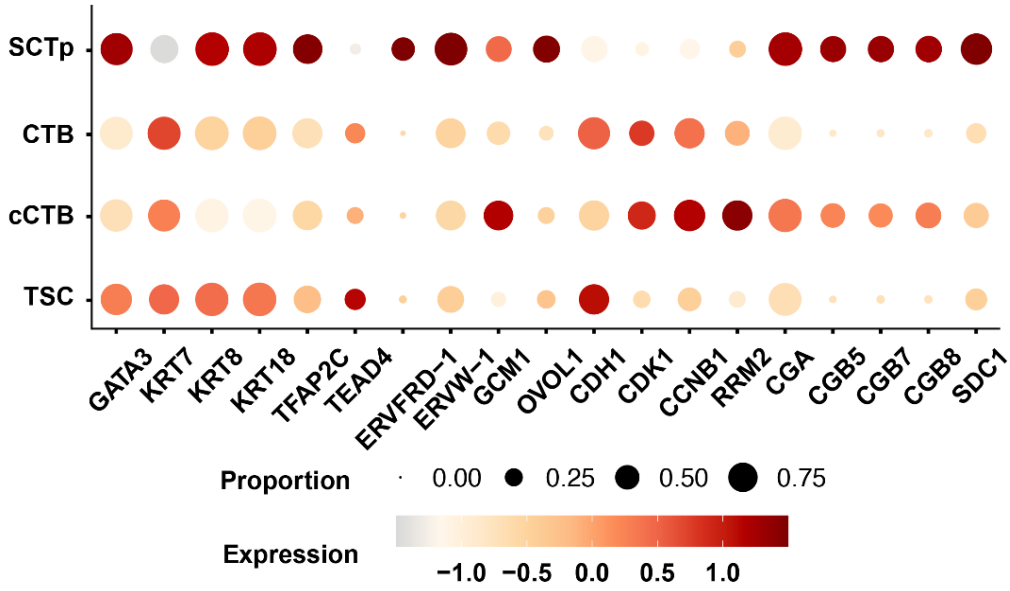

Figure S12. The expression of trophoblast marker genes in the trophoblast cells of competing models.

Dot plot indicating the expression of trophoblast marker genes in the scRNA-seq data of competing trophoblast organoids. SCTp, syncytiotrophoblast precursors. cCTB, column CTB-like cell. TSC, trophoblast stem cell.

Figure S13

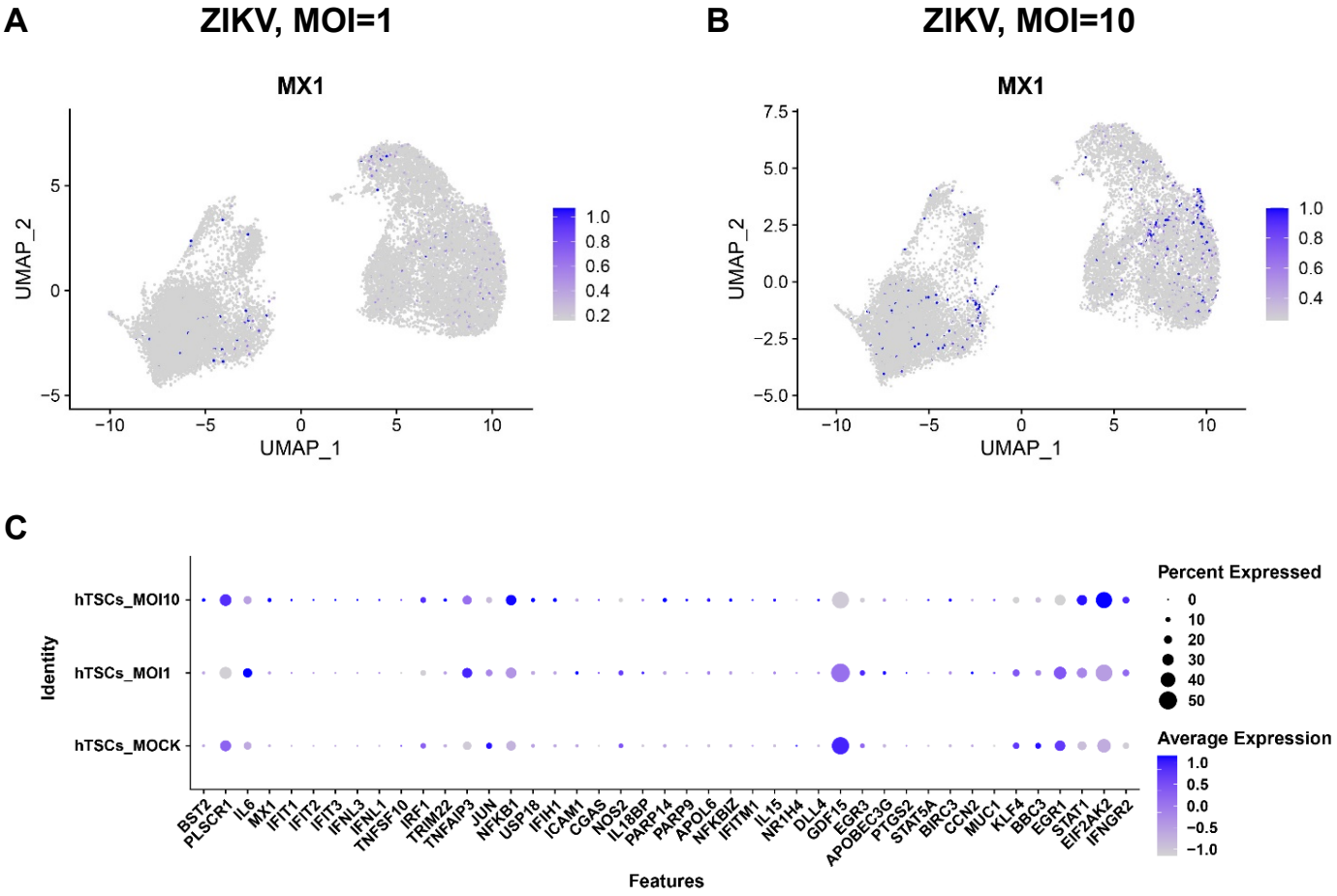

Figure S13. The expression of IFNs in MX1-positive cells of ZIKV-infected hTSC-organoids.

(A and B) UMAP showing the MX1-positive cells in the hTSC-organoids infected by ZIKV at an MOI of 1 (panel A) and 10 (panel B).

(C) Dot plot indicating the expression of the IFNs in the hTSCs from mock- and ZIKV (MOI 1 and 10)-infected hTSC-organoids.

Figure S14

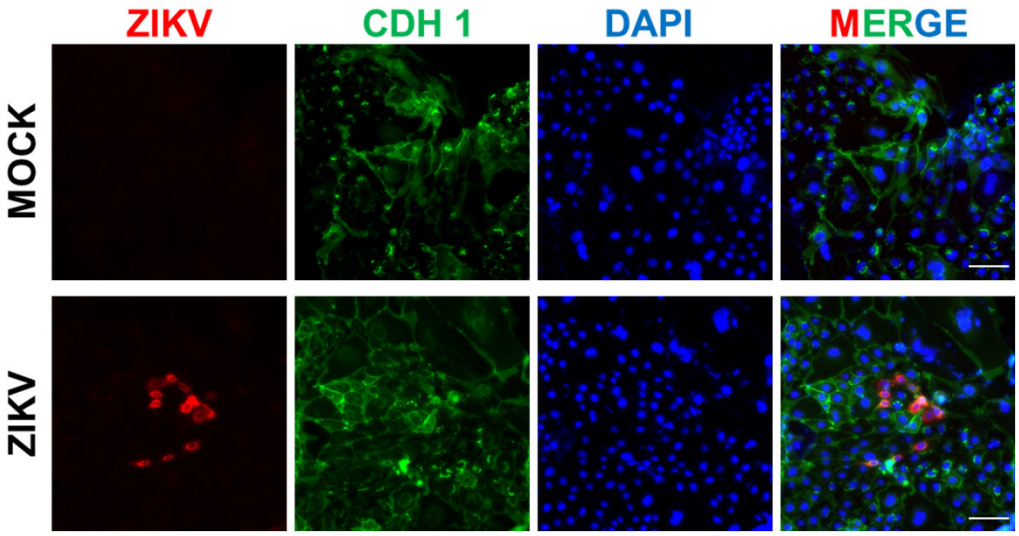

Figure S14. Immunofluorescence staining for ZIKV and CDH 1 in STB^{TS}.
Immunofluorescence staining for ZIKV and CDH 1 in STB^{TS}. The hTSCs were infected with ZIKV at an MOI of 1 and induced to STB^{TS} and analyzed at 96 hours. The representative images were selected from three independent experiments. Nuclei were stained with DAPI. Scale bars: 100 μm.

Figure S15

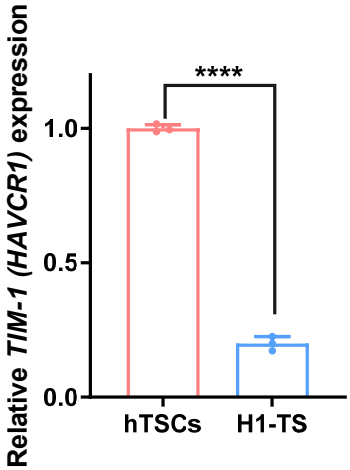

Figure S15. The expression of TIM-1 (HAVCR1) in blastocyst-derived hTSCs and hESC-derived hTSC-like cells.

Quantification of TIM-1 (HAVCR1) mRNA expression in blastocyst-derived hTSCs (hTSCs) and hESC-derived hTSC-like cells (H1-TS). Two-tailed unpaired t test was used for statistical analysis of significance. n=3 independent experiments. n=3 independent experiments. ****, $p<0.0001$. Data in this figure are shown as the mean ± s.d.

Table S1. Statistical results of ZIKV-positive cells in the hTSCs and STB^{TS} infected with ZIKV at 24 hpi.

	T	P	%
hTSCs	84	9	10.71429
	134	6	4.477612
	91	3	3.296703
	27	6	22.22222
	76	7	9.210526
	93	7	7.526882
	154	6	3.896104
	49	5	10.20408
	68	6	8.823529
	58	6	10.34483
STB^{TS}	65	3	4.615385
	86	5	5.813953
	103	3	2.912621
	140	6	4.285714

T, Total number of nuclei in the field; P, Number of ZIKA E-positive nuclei in the field; %, (P/T)×100.

Table S2. Statistical results of ZIKV-positive cells in the hTSCs, STB^{TS} and EVT^{TS} infected with ZIKV at 48 hpi.

	T	P	%
hTSCs	150	10	6.666667
	187	14	7.486631
	196	21	10.71429
	123	8	6.504065
	135	12	8.888889
	272	11	4.044118
	189	15	7.936508
	108	8	7.407407
	194	34	17.52577
	159	10	6.289308
STB^{TS}	140	4	2.857143
	175	14	8
	172	10	5.813953
	101	6	5.940594
	93	3	3.225806
	111	15	13.51351
	172	8	4.651163
	102	7	6.862745
EVT^{TS}	92	3	3.26087
	102	6	5.882353
	48	2	4.166667
	41	1	2.439024

T, Total number of nuclei in the field; P, Number of ZIKA E-positive nuclei in the field; %, (P/T)×100.

Table S3. Statistical results of the fusion index of the STB^{TS} differentiated from ZIKV-infected hTSCs.

N	S	T
80	9	303
63	7	319
54	10	280
97	9	283
31	9	371
58	6	488
72	7	311
47	10	382
42	8	304
46	8	246

N, Number of nuclei in syncytia; S, Number of syncytia; T, Total number of nuclei.

Table S4. Statistical results of the fusion index of the STB^{TS} differentiated from Mock-infected hTSCs.

N	S	T
79	12	230
61	10	281
82	11	253
115	9	221
32	8	232
59	7	212
72	8	209
59	10	198
62	10	272
75	9	225

N, Number of nuclei in syncytia; S, Number of syncytia; T, Total number of nuclei.

Table S5. Primers for qPCR and qRT-PCR.

Primer	Sequence (5'-3')
ZIKV-F	GGTCAGCGTCCTCTCTAATAAACG
ZIKV-R	GCACCCTAGTGTCCACTTTTTCC
ZIKV-Probe	FAM-AGCCATGACCGACACCACACCGT-BHQ1
AXL-RT-F	CCGTGGACCTACTCTGGCT
AXL-RT-R	CCTTGGCGTTATGGGCTTC
TIM-1-RT-F	TGGCAGATTCTGTAGCTGGTT
TIM-1-RT-R	AGAGAACATGAGCCTCTATTCCA
TYRO3-RT-F	CAGCCGGTGAAGCTCAACT
TYRO3-RT-R	TGGCACACCTTCTACCGTGA
MERTK-RT-F	CTCTGGCGTAGAGCTATCACT
MERTK-RT-R	AGGCTGGGTTGGTGAAAACA
GCM1-RT-F	TTCCCGGTCACCAACTTCTG
GCM1-RT-R	GTAAACTCCCCTGACTTTGTGTT
ERVW-1-RT-F	ATGCCCCGCAACTGCTATC
ERVW-1-RT-R	AGACAGTGACTCCAAGTCCTC
ERVFRD-1-RT-F	ACCGCCATCCTGATTTCCC
ERVFRD-1-RT-R	GAGGCTGGATAAGCTGTCCC
OVOL1-RT-F	TGAACATGAGCCTTCGAGACT
OVOL1-RT-R	CAAGGGTCACCTTCATCTTGG
HLA-G-RT-F	GAGGAGACACGGAACACCAAG
HLF-G-RT-R	GTCGCAGCCAATCATCCACT
miR-517-5p-RT-F	TCGGCAGGCCTCTAGATGGAAG
miR-526a-3p-RT-F	TCGGCAGGGAAAGCGCTTCCTT
miR-517a/b-3p-RT-F	TCGGCAGGATCGTGCATCCCTT
miR-526b-3p-RT-F	TCGGCAGGGAAAGTGCTTCCTT
miR-525-5p-RT-F	TCGGCAGGGAAGGCGCTTCCCT

RT, Real-time; F, Forward; R, Reverse.

Table S6. sgRNAs for gene knockout.

Primer	Sequence (5'-3')
AXL sgRNA-F	GGGGACTCACGGGCACCCTT
AXL sgRNA-R	AAGGGTGCCCGTGAGTCCCC
TIM-1 sgRNA-F	TCATGTCATTGAACCACCCA
TIM-1 sgRNA-R	TGGGTGGTTCAATGACATGA
TYRO3 sgRNA-F	CGGCCGGTACTGGTGCCAGG
TYRO3 sgRNA-R	CCTGGCACCAGTACCGGCCG
MERTK sgRNA-F	TAGGGGCTTTGATTCGACAG
MERTK sgRNA-R	CTGTCGAATCAAAGCCCCTA

F, Forward; R, Reverse.

Table S7. Primers for genotyping.

Primer	Sequence (5’-3’)
AXL-GT-F	AGCGCGACCTGTTAAGTCTC
AXL-GT-R	AGTGGTCAAACTGGGGTTCC
TIM-1-GT-F	CCACTACAGTGGAGCTGTCA
TIM-1-GT-R	AGGACTTACGGGAACCTCCTC
TYRO3-GT-F	AGTTGTACATCCCAGTCAGCG
TYRO3-GT-R	GCTCAAGCAACGGAAACAGA
MERTK-GT-F	CTTGAGCCCTGCTGTGTCAT
MERTK-GT-R	TGATGTGCCCCAAGCAATTC

GT, Genotyping; F, Forward; R, Reverse.

Table S8. qRT-PCR primers for detection of ISG expression

Primer (F, Forward; R, Reverse)	Sequence (5'-3')
IFI6-RT-F	GGTCTGCGATCCTGAATGGG
IFI6-RT-R	TCACTATCGAGATACTTGTGGGT
ODC1-RT-F	TTTACTGCCAAGGACATTCTGG
ODC1-RT-R	GGAGAGCTTTTAACCACCTCAG
LY6E-RT-F	CAGCTCGCTGATGTGCTTCT
LY6E-RT-R	CAGACACAGTCACGCAGTAGT
SAT1-RT-F	ACCCGTGGATTGGCAAGTTAT
SAT1-RT-R	TGCAACCTGGCTTAGATTCTTC
CDKN1A-RT-F	TGTCCGTCAGAACCCATGC
CDKN1A-RT-R	AAAGTCGAAGTTCCATCGCTC
EIF3L-RT-F	TGACCCCTACGCTTATCCCAG
EIF3L-RT-R	GTTTGCTGTTCATACTGACGTTC
MCL1-RT-F	TGCTTCGGAAACTGGACATCA
MCL1-RT-R	TAGCCACAAAGGCACCAAAAG
DDX3X-RT-F	AGCAGTTTTGGATCTCGTAGTG
DDX3X-RT-R	ACTGTTTCCACCACGTTCAAAT
ISG15-RT-F	CGCAGATCACCCAGAAGATCG
ISG15-RT-R	TTCGTCGCATTTGTCCACCA
IFNGR1-RT-F	TCTTTGGGTCAGAGTTAAAGCCA
IFNGR1-RT-R	TTCCATCTCGGCATACAGCAA
TNFAIP3-RT-F	TCCTCAGGCTTTGTATTTGAGC
TNFAIP3-RT-R	TGTGTATCGGTGCATGGTTTTA
IFIT1-RT-F	AGAAGCAGGCAATCACAGAAAA
IFIT1-RT-R	CTGAAACCGACCATAGTGGAAAT
IFIT2-RT-F	AAGCACCTCAAAGGGCAAAAC
IFIT2-RT-R	TCGGCCCATGTGATAGTAGAC
IFIT3-RT-F	AGAAAAGGTGACCTAGACAAAGC
IFIT3-RT-R	CCTTGTAGCAGCACCCAATCT
IFIT5-RT-F	GGCCAAAATAAAGACGCCCTT
IFIT5-RT-R	GACCAGGCTTCGTACTTCTTC
IFITM1-RT-F	CCAAGGTCCACCGTGATTAAC
IFITM1-RT-R	ACCAGTTCAAGAAGAGGGTGTT
IFITM2-RT-F	ATGAACCACATTGTGCAAACCT
IFITM2-RT-R	CCCAGCATAGCCACTTCCT
TLR3-RT-F	TTGCCTTGTATCTACTTTTGGGG
TLR3-RT-R	TCAACACTGTTATGTTTGTGGGT
TLR7-RT-F	TCCTTGGGGCTAGATGGTTTC
TLR7-RT-R	TCCACGATCACATGGTTCTTTG
IRF1-RT-F	ATGCCCATCACTCGGATGC
IRF1-RT-R	CCCTGCTTTGTATCGGCCTG
IRF2-RT-F	CATGCGGCTAGACATGGGTG
IRF2-RT-R	GCTTTCCTGTATGGATTGCCC
IRF7-RT-F	GCTGGACGTGACCATCATGTA
IRF7-RT-R	GGGCCGTATAGGAACGTGC
IRF9-RT-F	GCCCTACAAGGTGTATCAGTTG
IRF9-RT-R	TGCTGTCGCTTTGATGGTACT
IFIH1-RT-F	TCGAATGGGTATTCCACAGACG
IFIH1-RT-R	GTGGCGACTGTCCTCTGAA
MX1-RT-F	GTTTCCGAAGTGGACATCGCA
MX1-RT-R	CTGCACAGGTTGTTCTCAGC
EPSTI1-RT-F	ACCCGCAATAGAGTGGTGAAC
EPSTI1-RT-R	GCTATCAAGGTGTATGCACTTGT
OAS1-RT-F	TGTCCAAGGTGGTAAAGGGTG
OAS1-RT-R	CCGGCGATTTAACTGATCCTG
OAS2-RT-F	CTCAGAAGCTGGGTTGGTTTAT
OAS2-RT-R	ACCATCTCGTCGATCAGTGTC
OAS3-RT-F	GAAGGAGTTCGTAGAGAAGGCG

OAS3-RT-R	CCCTTGACAGTTTTCAGCACC
OASL-RT-F	CTGATGCAGGAACTGTATAGCAC
OASL-RT-R	CACAGCGTCTAGCACCTCTT
APOL1-RT-F	TGGACTACGGAAAGAAGTGGT
APOL1-RT-R	CCTCCTTCAATTTGTCAAGGCTT
APOL6-RT-F	ACCAGGCGGAGAGAGAAAGT
APOL6-RT-R	TGTAGCTCCACGTCTTCACAC
IFI27-RT-F	TGCTCTCACCTCATCAGCAGT
IFI27-RT-R	CACAACTCCTCCAATCACAACT
PARP12-RT-F	GCTTGACAACCGAACACAACC
PARP12-RT-R	GGCATAGCTCATTATAGCTCAGG
EIF2AK2-RT-F	GCCGCTAAACTTGCATATCTTCA
EIF2AK2-RT-R	TCACACGTAGTAGCAAAAGAACC
IFITM3-RT-F	TGTCCAAACCTTCTTCTCTCC
IFITM3-RT-R	CGTCGCCAACCATCTTCC
PNPT1-RT-F	GCGAGCACTATGGAGTAGCG
PNPT1-RT-R	GCAGTGTCACCTGACTGTACTA
PABPC4-RT-F	AAGCCAATCCGCATCATGTG
PABPC4-RT-R	CTCTTGGGTCTCGAAGTGGAC
CREB3L3-RT-F	ATGAATACGGATTTAGCTGCTGG
CREB3L3-RT-R	AGGAAGTCGTCAGAGTCGGG
MT1G-RT-F	CTTCTCGCTTGGGAACTCTA
MT1G-RT-R	AGGGGTCAAGATTGTAGCAAA
MT1H-RT-F	ATCTGCAAAGGGGCGTCAG
MT1H-RT-R	GAATGTAGCAAATGAGTCGGAGTT
MT1F-RT-F	GAATGTAGCAAATGGGTCAAGGTG
MT1F-RT-R	TCTCCTGCACCTGCGCTGGT
MT1X-RT-F	GACCCCAACTGCTCCTGCTCG
MT1X-RT-R	GATGTAGCAAACGGGTCAGGGTTGTAC